NeuroImage: Clinical 31 (2021) 102717

Contents lists available at ScienceDirect

NeuroImage: Clinical

journal homepage: www.elsevier.com/locate/ynicl

Oh brother, where art tau? Amyloid, neurodegeneration, and cognitive decline without elevated tau

Lauren E. McCollum [a,b,*], Sandhitsu R. Das [a,c], Long Xie [c], Robin de Flores [a,c,d], Jieqiong Wang [a], Sharon X. Xie [e], Laura E.M. Wisse [c,f], Paul A. Yushkevich [c], David A. Wolk [a], for the Alzheimer's Disease Neuroimaging Initiative

[a] Department of Neurology, University of Pennsylvania, Philadelphia, PA, USA
[b] Department of Medicine, University of Tennessee Graduate School of Medicine, Knoxville, TN, USA
[c] Department of Radiology, Penn Image Computing and Science Laboratory (PICSL), University of Pennsylvania, Philadelphia, PA, USA
[d] INSERM UMR-S U1237, Université de Caen Normandie, Caen, Normandy, USA
[e] Department of Biostatistics, Epidemiology, and Informatics, University of Pennsylvania, Perelman School of Medicine, Philadelphia, PA, USA
[f] Department of Diagnostic Radiology, Lund University, Lund, Sweden

ARTICLE INFO

Keywords:
Mild cognitive impairment
Alzheimer's disease
Tau
Amyloid
Biomarkers

ABSTRACT

Mild cognitive impairment (MCI) can be an early manifestation of Alzheimer's disease (AD) pathology, other pathologic entities [e.g., cerebrovascular disease, Lewy body disease, LATE (limbic-predominant age-related TDP-43 encephalopathy)], or mixed pathologies, with concomitant AD- and non-AD pathology being particularly common, albeit difficult to identify, in living MCI patients. The National Institute on Aging and Alzheimer's Association (NIA-AA) A/T/(N) [β-Amyloid/Tau/(Neurodegeneration)] AD research framework, which classifies research participants according to three binary biomarkers [β-amyloid (A+/A-), tau (T+/T-), and neurodegeneration (N+/N-)], provides an indirect means of identifying such cases. Individuals with A+T-(N+) MCI are thought to have both AD pathologic change, given the presence of β-amyloid, and non-AD pathophysiology, given neurodegeneration without tau, because in typical AD it is tau accumulation that is most tightly linked to neuronal injury and cognitive decline. Thus, in A+T-(N+) MCI (hereafter referred to as "mismatch MCI" for the tau-neurodegeneration mismatch), non-AD pathology is hypothesized to drive neurodegeneration and symptoms, because β-amyloid, in the absence of tau, likely reflects a preclinical stage of AD. We compared a group of individuals with mismatch MCI to groups with A+T+(N+) MCI (or "prodromal AD") and A-T-(N+) MCI (or "neurodegeneration-only MCI") on cross-sectional and longitudinal cognition and neuroimaging characteristics. β-amyloid and tau status were determined by CSF assays, while neurodegeneration status was based on hippocampal volume on MRI. Overall, mismatch MCI was less "AD-like" than prodromal AD and generally, with some exceptions, more closely resembled the neurodegeneration-only group. At baseline, mismatch MCI had less episodic memory loss compared to prodromal AD. Longitudinally, mismatch MCI declined more slowly than prodromal AD across all included cognitive domains, while mismatch MCI and neurodegeneration-only MCI declined at comparable rates. Prodromal AD had smaller baseline posterior hippocampal volume than mismatch MCI, and whole brain analyses demonstrated cortical thinning that was widespread in prodromal AD but largely restricted to the medial temporal lobes (MTLs) for the mismatch and neurodegeneration-only MCI groups. Longitudinally, mismatch MCI had slower rates of volume loss than prodromal AD throughout the MTLs. Differences in cross-sectional and longitudinal cognitive and neuroimaging measures between mismatch MCI and prodromal AD may reflect disparate underlying pathologic processes, with the mismatch group potentially being driven by non-AD pathologies on a background of largely preclinical AD. These findings suggest that β-amyloid status alone in MCI may not reveal the underlying driver of symptoms with important implications for enrollment in clinical trials and prognosis.

* Corresponding author at: The Pat Summitt Clinic, University of Tennessee Medical Center, 1932 Alcoa Highway, Building C, Suite 150, Knoxville, TN 37920, USA.
E-mail address: lemccollum@utmck.edu (L.E. McCollum).

https://doi.org/10.1016/j.nicl.2021.102717
Received 6 October 2020; Received in revised form 21 May 2021; Accepted 2 June 2021
Available online 6 June 2021

1. Introduction

Mild cognitive impairment (MCI) is a clinical diagnosis defined by objective cognitive impairment, accompanied by concern for cognitive change (voiced by the patient or a knowledgeable informant), with relative preservation of functional independence (Petersen, 2016). Though MCI was initially described as an intermediary state between normal aging and Alzheimer's disease (AD) dementia, AD pathology is just one of many processes that can underlie MCI (Petersen, 2016). Other causes of MCI include cerebrovascular disease, psychiatric disease (especially depression), and various non-AD neurodegenerative pathologies, such as frontotemporal lobar degeneration, Lewy body disease, limbic-predominant age-related TDP-43 encephalopathy (LATE), hippocampal sclerosis, primary age-related tauopathy (PART), and others (Petersen, 2004, 2016; Jicha et al., 2006; Carrière et al., 2009; Pillai et al., 2016; Abner et al., 2017; Nelson et al., 2019). Increasingly, there has been recognition that, even though AD pathology remains among the most common underlying pathologic findings in MCI, the pathology is very often mixed, and a particularly common scenario is the combination of AD pathology and non-AD pathology (Abner et al., 2017). Variations in the types, amounts, and temporal distribution of concomitant non-AD pathologies may account for a great deal of the heterogeneity of MCI (Boyle et al., 2017).

Clinicians and researchers are faced with the task of inferring the underlying causes of MCI in individuals. In clinical settings, knowledge of the underlying pathology aids in both treatment and prognostication. Assuring the same underlying pathology is of particular importance in clinical trials that target the molecular pathology of AD. Improvements in *in vivo* biomarkers have helped with this, but there are several limitations. Hippocampal neurodegeneration on volumetric MRI is a commonly used structural biomarker that suggests the presence of AD pathology but is non-specific (Gordon et al., 2016). Abnormal accumulation of β-amyloid, which can be ascertained by amyloid PET or β-amyloid 1–42 (Aß42) in CSF, is specific for AD pathology, but because amyloid accumulation begins years before clinical symptom onset, it is also a common finding in asymptomatic individuals (Jack et al., 2017). Elevated phosphorylated-tau-181 (p-tau) in CSF and abnormal tau PET scans are difficult to interpret outside of the context of an abnormal β-amyloid biomarker (Jack et al., 2018). None of these commonly used AD biomarkers can confirm or exclude the possibility of concomitant non-AD pathologies. While cerebrovascular disease can be suggested by the presence of chronic lacunar infarcts or white matter hyperintensities (WMHs) on MRI of the brain, most non-AD neurodegenerative pathologies lack reliable biomarkers (Prins and Scheltens, 2015). At this time, it is very challenging to identify specific non-AD neurodegenerative pathologies in living individuals.

The National Institute on Aging and Alzheimer's Association (NIA-AA) "A/T/(N)" [β-amyloid/Tau/(Neurodegeneration)] AD research framework is a system for conceptualizing AD biomarkers that may provide an alternative, indirect approach for identifying instances of combined AD and non-AD disease pathology (Jack et al., 2018). In this framework, individuals are classified at each timepoint according to three binary biomarkers: β-amyloid (A+/A-), tau (T+/T-), and neurodegeneration (N+/N-). The expected progression of classical "pure" AD through this biomarker schema is (1) asymptomatic development of amyloid elevation without tau or neurodegeneration [A+T-(N-)], followed, often years later, by (2) pathologic accumulation of tau [A+T+(N-)], and, finally, (3) neuronal injury and neurodegeneration [A+T+(N+)]. Clinical MCI or dementia, per the model, does not occur until all three biomarkers are abnormal. However, biomarker combinations that do not appear in this typical sequence do occur and may be indicative of other processes. For instance, the biomarker combination A+T-(N+) is thought to signify both AD and non-AD pathology. β-Amyloid signifies AD pathologic change, while neurodegeneration in the absence of tau, which is thought to be directly linked to neurodegeneration in AD, suggests a non-AD driver of neuronal injury.

In this study, we examined a group of individuals with A+T-(N+) MCI (hereafter referred to as "mismatch MCI," for the mismatch between tau and neurodegeneration) from the Alzheimer's Disease Neuroimaging Initiative (ADNI) using CSF-based biomarkers for β-amyloid and tau (p-tau) and structural MRI for neurodegeneration. While the A/T/(N) framework does allow the use of CSF total tau (t-tau) as a biomarker for neurodegeneration, CSF t-tau has been found to be highly correlated with CSF p-tau and less sensitive for detection of suspected non-AD pathologies than other markers of neurodegeneration (Cousins et al., 2021); thus, hippocampal volume on structural MRI was instead chosen as the neurodegeneration biomarker in this study. We believe the mismatch group consists of individuals whose cognitive decline and atrophy are driven by concomitant non-AD pathologies rather than their AD pathologic change, which is expected to be in a preclinical state, as it is unlikely to cause symptoms in the absence of neurofibrillary tangle pathology. We compared cross-sectional and longitudinal cognition and imaging characteristics of mismatch MCI to A+T+(N+) MCI, hereafter referred to as "prodromal AD," to investigate whether mismatch MCI differed from prodromal AD in ways that may be best explained by the presence of concomitant AD and non-AD pathology. We predicted that the mismatch MCI group would be less "AD-like" than the prodromal AD group with regard to baseline cognitive profiles and imaging characteristics, reflecting the hypothesis that non-AD pathology is driving cognitive impairment and neurodegeneration in the absence of tau. Specifically, we hypothesized that mismatch MCI would have less baseline episodic memory impairment and more executive function impairment than prodromal AD, as typical AD usually begins with marked memory loss out of proportion to other domains, while cerebrovascular disease (a particularly common non-AD pathology) typically affects executive function (Mendez et al., 1997). We also compared mismatch MCI to A-T-(N+) MCI ("neurodegeneration-only MCI"), as this group is also thought to have non-AD drivers of neurodegeneration, given the absence of amyloid, and, therefore, might be expected to display similar characteristics. We hypothesized that mismatch MCI and neurodegeneration-only MCI would have similar cognitive profiles at baseline because they likely have comparable underlying pathologies driving neurodegeneration and cognitive impairment. For the longitudinal analysis of cognition, we predicted that mismatch MCI would exhibit cognitive decline at rates that were slower than prodromal AD and comparable to neurodegeneration-only MCI. Amyloid-negative cognitively normal (A- CN) participants were included as a control group.

With regard to neuroimaging, we hypothesized that, at baseline, mismatch MCI would have less cortical thinning in AD signature regions (e.g., posterior parietal lobes) (Dickerson et al., 2009) compared to prodromal AD, and that cortical thinning patterns would be similar between mismatch MCI and neurodegeneration-only MCI. Longitudinally, we hypothesized that mismatch MCI would have slower rates of atrophy in the hippocampus and extrahippocampal medial temporal lobe (MTL) regions compared to prodromal AD and that mismatch MCI and neurodegeneration-only MCI would have comparable rates of atrophy.

2. Materials and methods

2.1. Participants

Data used in this study were obtained from ADNI (adni.loni.usc.edu). ADNI was launched in 2003 as a public–private partnership, led by Principal Investigator Michael W. Weiner, MD. The primary goal of ADNI has been to test whether serial MRI, PET, other biological markers, and clinical and neuropsychological assessment can be combined to measure the progression of MCI and early AD. For up-to-date information, see www.adni-info.org.

Participants were recruited at sites throughout the United States and Canada within ADNI during the ADNI-2 and ADNI-GO phases of the

study. Baseline ages ranged from 55 to 90 years old. Participants were English- or Spanish-speaking, non-depressed, in good general health, and had baseline diagnoses of cognitively normal (CN), MCI, or AD dementia. Participants with MCI or dementia had a subjective memory complaint (voiced by the subject, the study partner, or the clinician), objective evidence of memory dysfunction (based on the Logical Memory II subscale score from the Weschler Memory Scale – Revised), and a Modified Hachinski Ischemic Score of 4 or less, indicating that a vascular etiology for the cognitive impairment is less likely. Patients with non-amnestic presentations or an existing diagnosis of multi-infarct dementia were excluded from ADNI. All selected participants underwent lumbar puncture for CSF-based AD biomarkers, a venipuncture for ApoE genotyping, structural 3 T MRI, and cognitive testing during the screening and baseline period. See http://adni.loni.usc.edu/ for a full description of the ADNI study protocols.

2.2. Standard protocol approvals, registrations, and patient consents

All participants gave written informed consent per the ADNI-2 (NCT0123197) or ADNI-GO (NCT01078636) protocols. Study procedures were approved by each study site's institutional review board.

2.3. CSF acquisition and processing

Participants underwent fasting lumbar puncture at baseline and every other year thereafter, as participant willingness allowed. Under sterile conditions, site medical personnel collected from each participant 20 mL of CSF, 2 mL of which was sent to each site's local lab for routine studies (cell counts, protein, and glucose) and the remainder of which was sent to the Penn AD Biomarker Fluid Bank Laboratory, where assays for Aß42, p-tau, and t-tau were performed (Shaw et al., 2009, 2011; Bittner et al., 2016).

2.4. A/T/(N) biomarker status determination and group formation

CSF was processed with the Roche Elecsys platform (Blennow et al., 2019). β-amyloid status was determined by a cut-off of Aß42 of 980 picograms (pg) per milliliter (mL) in CSF, such that those below this cutoff were considered positive (A+) and equal to or above were considered negative (A-)(Shaw). Tau status was defined by a cut-off of p-tau of 24 pg/mL, such that above and equal to this cutoff constituted positive (T+) individuals while below were negative (T-)(Shaw; Blennow et al., 2019). Neurodegeneration positivity (N+) was defined as intracranial-volume- and age-adjusted mean hippocampal volume less than or equal to the 90th percentile hippocampal volume of 111 amyloid-positive individuals with a diagnosis of AD dementia (3171 mm^3), as has been done in similar analyses (Jack et al., 2012; Wisse et al., 2015). (See section 2.6 for description of volumetric MRI methods.)

Using these cut-offs, a total of 401 participants with MCI were classified according to A/T/(N) biomarker status, and 176 of them fell into one of the three MCI groups included in the study. The baseline MCI groups consisted of 44 individuals with mismatch MCI (11.0% of total MCI cases), 84 with prodromal AD (20.9% of total MCI cases), and 48 with neurodegeneration-only MCI (12.0% of total MCI cases). Additionally, there were 161 A- CN controls. Membership in the A- CN control group was not restricted by tau or neurodegeneration status. Longitudinal analyses of cognition included everyone in the three MCI groups and the A- CN control group who underwent at least one follow-up neuropsychological battery at 12, 24, 36, or 48 months. These analyses included 43 individuals with mismatch MCI, 77 with prodromal AD, 45 with neurodegeneration-only MCI, and 152 A- CN. The longitudinal imaging analysis included 34 individuals in mismatch MCI, 61 in prodromal AD, 37 in neurodegeneration-only MCI, and 141 in A- CN.

Participants were kept in their original baseline groups for the longitudinal analyses, regardless of whether their clinical diagnosis or biomarker status changed, as the intention was to compare the trajectory of people with mismatch MCI at baseline to the other groups. Post-hoc analyses were performed to investigate the extent to which participants in the T- MCI groups (mismatch MCI and neurodegeneration MCI) progressed to T + MCI, based on CSF p-tau or tau PET, during follow-up.

2.5. Cognitive assessments

Study participants underwent psychometric testing at baseline and annually thereafter. Cognitive measures included the Rey Auditory Verbal Learning Test (RAVLT), the Animal Naming Test, and the Trail Making Test to assess memory, language, and executive function, respectively. During the RAVLT, the tester reads aloud a 15-word list to the participant over five consecutive trials. After each trial, the participant repeats back as many of the words as possible (Moradi et al., 2017). After a distraction task, the participant is asked to recall the words, and the number of correct responses is the 5-minute delayed recall score. In this study, immediate memory and episodic memory were assessed using the first trial and 5-minute delayed recall trial, respectively.

The Animal Naming Test is a test of category fluency (Binetti et al., 1995). Participants are given one minute to name as many animals as they can. The Trail Making Test consists of two parts – Trails A and Trails B. In Trails A, participants "connect the dots" between 25 circled numbers in consecutive order on paper; in Trails B, participants alternate between letters and numbers (1, A, 2, B, 3, C, etc.) (Tombaugh, 2004). The score for each test is the time in seconds for completion. Here, executive function was evaluated by calculating the difference between the completion times for Trails B and Trails A. Subtraction of Trails A time from Trails B time controls for processing speed, and the resulting difference is a more accurate reflection of executive function, than Trails B time alone (Corrigan and Hinkeldey, 1987).

The Mini Mental State Exam (MMSE) and Geriatric Depression Scale (GDS) were administered to participants as part of their baseline assessment.

2.6. Neuroimaging measures

Participants underwent structural MRI scans acquired on 3 T scanners at screening, 3 months, 6 months, 12 months, and annually thereafter. Up-to-date information about MRI imaging protocols can be found at adni.loni.usc.edu/methods/mri-tool/mri-analysis. MRI scans were uploaded to LONI (the Laboratory for Neuroimaging). Quality control was performed by the MRI Core at the Mayo Clinic.

Baseline MTL subregional measures were obtained from baseline MRI scans using automated segmentation from the tailored pipeline, Automatic Segmentation of Hippocampal Subfields-T1 (ASHS-T1) (Yushkevich et al., 2015; Xie et al., 2017, 2019). This pipeline provided volumes of the whole hippocampus, anterior hippocampus, and posterior hippocampus and cortical thickness measures of entorhinal cortex (ERC), Brodmann area 35 (BA35), Brodmann area 36 (BA36), and parahippocampal cortex (PHC). The right- and left-sided volumes and thicknesses were averaged for analyses. An anterior-to-posterior-hippocampal-volume ratio was also calculated, given prior work suggesting that this ratio may be associated with the presence of TDP-43 pathology (de Flores et al., 2020). WMH volumes, which were downloaded from the ADNI website, were quantified via an automated detection method that utilized T1-, T2-, and proton-density weighted MRI images, as previously described (Schwarz et al., 2009; Dadar et al., 2017).

Whole-brain cortical thickness maps were constructed from baseline T1-weighted MRI images using a method based on diffeomorphic registration (Das et al., 2009), which was implemented in the Advanced Normalization Tools (ANTs) Cortical Thickness Pipeline (Tustison et al., 2014; Wolk et al., 2017). Cortical thickness comparison maps were generated to demonstrate areas of significant difference between each

MCI group and A- CN and between mismatch MCI and the other two MCI groups. Overlap maps were generated to depict mismatch MCI's overlap of control-referenced cortical thinning with prodromal AD and neurodegeneration-only MCI, respectively.

The longitudinal imaging analysis of MTL subregion and WMH volumes included scans that occurred up to 4.5 years from baseline for each participant whose first and last MRI scans were at least 1.2 years apart. The volumes of each region in follow-up scans were estimated using Automatic Longitudinal Hippocampal Atrophy (ALOHA) software, which is an unbiased registration-based longitudinal pipeline (Das et al., 2012).

Exploratory analyses using baseline amyloid PET and the first tau PET scan (performed, on average, more than 5 years from baseline, based on the timing of incorporation of tau PET scans into the ADNI protocol) were also pursued using publicly available processed PET data from ADNI that included a composite measure of florbetapir PET and flortaucipir uptake in regions akin to Braak staging (Braak and Braak, 1991; Landau et al., 2015; Schöll et al., 2016). Details regarding image acquisition for florbetapir and flortuacipir PET are available on the ADNI website (http://adni.loni.usc.edu/). An additional group of amyloid-positive cognitively normal individuals (A+ CN, hereafter referred to as "preclinical AD," with A status defined by CSF criteria, as above) was included in this post-hoc analysis in order to test the hypothesis that the mismatch MCI group and the preclinical AD group would have similar tau burden.

2.7. Statistical analysis

Statistical analyses were conducted using SPSS version 26. Mean age at baseline MRI and years of education of mismatch MCI were compared to each of the other three groups using independent samples t-tests. All statistical tests were two-sided, and statistical significance was set at a level of < 0.05. Sex and ApoE4 carrier status (zero ApoE4 alleles versus one or two ApoE4 alleles) were compared between mismatch MCI and each of the three other groups using Pearson chi-square analyses. Median MMSE, GDS, and length of follow-up were compared between mismatch MCI and the other three groups using the Mann-Whitney U-Test for non-parametric analysis.

Z-scores, referenced to baseline performance of 161 A- CN controls, were calculated for each participant's baseline performance on the RAVLT trial 1, RAVLT 5-minute delayed recall, and the animal naming test as measures of immediate memory, episodic memory, and category fluency, respectively. To quantify executive function, Trails-B-minus-Trails-A time was calculated, and the natural log was taken to provide a more normal distribution, allowing for parametric analyses. Control-referenced Z-scores were calculated for each participant's natural log Trails-B-minus-Trails-A time, and the negative of this Z-score is reported in order to make the results more easily comparable to the other cognitive domains – i.e., the more negative the Z-score for each cognitive measure, the poorer the performance. Baseline cognition Z-scores were adjusted for age, sex, and education using unstandardized beta coefficients from linear regression analyses of A- CN. Mean adjusted baseline cognition Z-scores are reported for each group. The mean adjusted Z-score for each cognitive domain of mismatch MCI was compared to each of the other three groups using independent-sample t-tests.

Mean baseline Aß42, p-tau, and t-tau levels in CSF were compared between mismatch MCI and the three other groups using independent sample t-tests. The mean volumes of the hippocampus, anterior hippocampus, and posterior hippocampus were adjusted for age and intracranial volume using unstandardized beta coefficients from linear regression analysis of 161 A- CN. Mean cortical thickness values for extrahippocampal MTL regions (ERC, BA35, BA36, and PHC) were, similarly, adjusted for age. WMH volume was log-transformed to provide a more normal distribution and adjusted for age and intracranial volume using unstandardized beta coefficients from a linear regression analysis of the 140 A- CN for whom these data were available. The mean values for each of these structural measures and log WMH volume for mismatch MCI were compared to each of the other groups using independent sample t-tests.

Cortical thickness maps comparing each MCI group to A- CN and mismatch MCI to each of the other two MCI groups used familywise-error- (FWE)- corrected p-values, based on the Threshold-Free Cluster Enhancement (TFCE) method (Smith and Nichols, 2009), with a significance threshold of 0.05, with age, sex, and education as covariates.

Linear mixed-effects models were used to compare rates of change in cognition and longitudinal volumes of anterior and posterior hippocampus, ERC, BA35, BA36, PHC, and log WMH. For the cognitive measures, Z-scores (referenced to baseline performance of 161 A- CN) from all baseline and annual follow-up neuropsychological batteries performed at or before the 48-month visit for each participant were computed. Linear mixed effects models incorporating baseline age, sex, education, baseline unadjusted Z-scores, group, time, and time*group interaction as fixed effects were run for each cognitive domain's baseline and longitudinal unadjusted Z-scores between all four participant groups to generate graphical representations of the longitudinal change in each cognitive domain. For the longitudinal analysis of volume change in the selected MTL regions, mixed effects models incorporated baseline age, baseline volume, group, time, and time*group interaction as fixed effects. Additional linear mixed-effects models that compared mismatch MCI to each of the other three groups individually were run in order to determine differences in rates of cognitive decline, MTL region volume change, and WMH volume change. For each linear mixed effects model, a random intercept term was included to account for correlations among repeated measures.

The number of participants in mismatch MCI and neurodegeneration-only MCI who were deemed T+ at 24 and 48 months was compared using Fisher exact tests amongst those who underwent repeat lumbar puncture (LP) at these time points.

Tau and amyloid PET mean standardized uptake value ratios (SUVRs) for mismatch MCI, as well as mean number of years between baseline assessment and tau PET scan, were compared to those of the other participant groups using independent sample t-tests.

3. Results

3.1. Participant characteristics

Table 1 displays baseline characteristics of mismatch MCI, prodromal AD, neurodegeneration-only MCI, and A- CN controls. With a mean age of 70.8 ± 6.8 years, mismatch MCI was significantly younger than prodromal AD (73.3 ± 6.5 years, $p = 0.047$), but did not significantly differ in age from the other groups. Mismatch MCI had a significantly greater percentage of males (75%) than A- CN and prodromal AD ($p = 0.002$). The percentage of ApoE4 carriers for mismatch MCI (54.5%) was higher than that of A- CN (20.5%, $p < 0.001$) and neurodegeneration-only MCI (22.9%, $p = 0.002$) but lower than that of prodromal AD (77.4%, $p = 0.008$). Mismatch MCI's median GDS score did not differ significantly from the other two MCI groups.

3.2. Cross-sectional analyses

3.2.1. Baseline cognition

Table 2 displays baseline age-, sex-, and education-adjusted Z-scores for cognitive measures. Compared to A- CN, mismatch MCI had lower mean adjusted Z-scores on all included cognitive domains ($p \leq 0.001$). Compared to the other MCI groups, mismatch MCI had comparably impaired performance on immediate memory and category fluency. Regarding episodic memory, mismatch MCI was less impaired (−1.06 ± 0.84) than prodromal AD (−1.46 ± 0.93, $p = 0.019$) but more impaired than neurodegeneration-only MCI (−0.55 ± 0.93, $p = 0.007$). In the executive function domain, mismatch MCI and prodromal AD were

Table 1
Baseline demographic and clinical characteristics.

	Mismatch MCI (n = 44)	Prodromal AD (n = 84)	Neurodegeneration-only MCI (n = 48)	A- CN (n = 161)
Age at baseline MRI [mean ± SD (p-value)][a]	70.8 ± 6.8	73.3 ± 6.5 (0.047*)	69.7 ± 7.3 (0.464)	72.3 ± 6.1 (0.178)
Years of education [mean ± SD (p-value)][a]	16.5 ± 2.8	16.0 ± 2.7 (0.299)	16.4 ± 2.8 (0.914)	16.7 ± 2.6 (0.661)
Sex [% male, n (p-value)][b]	75.0, 33	46.4, 39 (0.002*)	56.3, 27 (0.059)	48.4, 78 (0.002*)
ApoE4 [% with 1 or 2 alleles, n (p-value)][b]	54.5, 24	77.4, 65 (0.008*)	22.9, 11 (0.002*)	20.5, 33 (<0.001*)
MMSE [median, IQR (p-value)][c]	29, 28–30	27, 26–29 (0.004*)	29, 28–30 (0.875*)	29, 29–30 (0.004*)
GDS [median, IQR (p-value)][c]	2, 1–2	1, 1–2 (0.324)	1, 1–2 (0.319)	0, 0–1 (<0.001*)
Length of follow-up in months [median, IQR (p-value)][c]	48, 24–48	36, 24–48 (0.268)	48, 36–60 (0.260)	24, 24–48 (0.013*)

All p-values reflect comparisons with the mismatch MCI group. a. data compared using Independent Samples T Test. b. data compared using Pearson Chi-Square test. c. data compared using Mann-Whitney U Test. SD, standard deviation; MMSE, Mini Mental State Exam; IQR, interquartile range; GDS, Geriatric Depression Scale; mismatch MCI, A+T-(N+) MCI; prodromal AD, A+T+(N+) MCI; neurodegeneration-only MCI, A-T-(N+) MCI; A- CN, amyloid-negative cognitively normal controls. Higher scores on GDS indicate more depressive symptoms. Length of follow-up is determined based on the last follow-up visit completed for each participant. *p < 0.05.

Table 2
Baseline age-, sex-, and education-adjusted Z-scores for cognition.

	Mismatch MCI (n = 44)	Prodromal AD (n = 84)	Neurodegeneration-only MCI (n = 48)	A- CN (n = 161)
Immediate memory	−0.59 ± 0.74	−0.80 ± 0.84 (0.166)	−0.46 ± 0.70 (0.375)	0.00 ± 0.93 (<0.001*)
Episodic memory	−1.06 ± 0.84	−1.46 ± 0.93 (0.019*)	−0.55 ± 0.93 (0.007*)	0.00 ± 0.91[a] (<0.001*)
Category fluency	−0.56 ± 1.11	−0.88 ± 0.92 (0.091)	−0.32 ± 0.87 (0.237)	0.00 ± 0.92 (0.001*)
Executive function	−0.93 ± 0.93[b]	−0.77 ± 1.17[c] (0.419)	−0.32 ± 0.72[d] (0.001*)	0.00 ± 0.97 (<0.001*)

Data presented as mean ± standard deviation (p-value) and compared to mismatch MCI group with Independent Sample T-Tests. Z scores are in reference to 161 A- CN. a. n = 160. b. n = 43. c. n = 82. d. n = 47. Mismatch MCI, A+T-(N +) MCI; prodromal AD, A+T+(N +) MCI; neurodegeneration-only MCI, A-T-(N+) MCI; A- CN, amyloid-negative cognitively normal controls. *p < 0.05.

similarly impaired at baseline, although mismatch MCI performed more poorly in absolute terms and was significantly more impaired (−0.93 ± 0.93) than neurodegeneration-only MCI (−0.32 ± 0.72, p = 0.001).

3.2.2. Baseline CSF and neuroimaging characteristics

Baseline CSF and neuroimaging characteristics are displayed in Table 3. As defined, the mismatch MCI and neurodegeneration-only MCI groups had lower CSF p-tau values than the prodromal AD group. Likewise, mismatch MCI did not differ from prodromal AD on CSF Aß42.

The age- and intracranial-volume-adjusted anterior hippocampal volume for mismatch MCI was similar to the other two MCI groups. However, the posterior hippocampal volume for mismatch MCI (1435.6 ± 162.5 mm^3) was significantly larger than that of prodromal AD (1350.7 ± 161.9 mm^3, p = 0.006) and similar to that of neurodegeneration-only MCI (1426.4 ± 137.9 mm^3, p = 0.768). The anterior-to-posterior-hippocampal-volume ratio for mismatch MCI (1.021 ± 0.142) did not statistically differ from that of A- CN and neurodegeneration-only MCI but was lower than that of prodromal AD (1.086 ± 0.144, p = 0.016). There were no significant differences between mismatch MCI and the other two MCI groups for the included extrahippocampal MTL regions (ERC, BA35, BA36, and PHC) at baseline. Compared to A- CN, mismatch MCI had lower mean cortical thickness for ERC, BA35 and PHC (p < 0.05). Age- and intracranial-volume-adjusted log WMH volume for mismatch MCI was comparable to that of prodromal AD but significantly higher than that of A- CN and neurodegeneration-only MCI (p < 0.05).

3.2.3. Baseline cortical thickness comparison maps

Whole brain voxel-wise cortical thickness maps comparing each of the three MCI groups to A- CN with a significance threshold of p < 0.05 (FWE-corrected) showed that mismatch MCI and neurodegeneration-only MCI demonstrated reduced cortical thickness that was relatively restricted to the MTL, while prodromal AD demonstrated more widespread areas of reduced cortical thickness that included both medial and lateral temporal cortices and parts of the frontal and parietal lobes (Fig. 1). Overlap maps showed that mismatch MCI's pattern of cortical thinning overlapped more with that of neurodegeneration-only MCI, which was similarly circumscribed, than with prodromal AD, which was more widespread (Fig. 1). Direct comparison of mismatch MCI to prodromal AD, using FWE-corrected p-values, demonstrated an area of significantly reduced cortical thickness in the left inferolateral temporal lobe for the prodromal AD group and no differences in the other direction (Supplemental Fig. 1). Comparison of mismatch MCI to neurodegeneration-only MCI using FWE-corrected p-values showed no significant differences in either direction. Comparison of mismatch MCI and prodromal AD using uncorrected p-values demonstrated widespread areas of decreased cortical thickness in prodromal AD compared to mismatch MCI, with only scant areas of decreased cortical thickness observed in mismatch MCI relative to prodromal AD (Supplemental Fig. 1).

3.3. Longitudinal analyses

3.3.1. Longitudinal cognition

Fig. 2 contains graphical representations of mixed effects models, incorporating baseline age, education, sex, baseline cognitive performance, group, time and time*group interaction as fixed effects, with p-values for time*group interaction terms for each cognitive domain's baseline and longitudinal Z-scores for all four participant groups, simultaneously. Supplemental Table 1 displays the time*group interaction term estimates, standard errors, and p-values in comparisons of mismatch MCI's baseline and longitudinal cognitive Z-scores to each of the other groups individually using mixed-effects models with the same parameters. Mismatch MCI and prodromal AD had significant time*-group interactions for all four cognitive domains (p < 0.05), reflecting a slower rate of decline in the former group. There were no significant time*group interactions between mismatch MCI and neurodegeneration-only MCI. The only domain in which mismatch MCI, in comparison to A- CN, had a significant time*group interaction was episodic memory (p < 0.032), reflecting faster decline in mismatch MCI in this domain. Supplemental Table 2 displays the number of participants in each group who underwent cognitive testing at baseline and at each year of follow-up.

3.3.2. Longitudinal neuroimaging

Fig. 3 represents mixed effects models comparing the four groups on

Table 3
Baseline CSF and neuroimaging characteristics.

	Mismatch MCI (n = 44)	Prodromal AD (n = 84)	Neurodegeneration-only MCI (n = 48)	A- CN (n = 161)
CSF t-tau (pg/mL)	183.5 ± 44.6	384.9 ± 122.9 (<0.001*)	191.8 ± 42.5 (0.364)	240.7 ± 88.8 (<0.001*)
CSF p-tau (pg/mL)	17.0 ± 4.8	38.9 ± 13.7 (<0.001*)	16.3 ± 3.7 (0.438)	21.3 ± 8.4 (<0.001*)
CSF Aß42 (pg/mL)	648.3 ± 212.5	666.7 ± 163.8 (0.617)	1493.1 ± 398.5 (<0.001*)	1721.2 ± 504.1 (<0.001*)
Hippocampal volume[a] (mm^3)	2891.1 ± 293.1	2803.8 ± 271.2 (0.095)	2857.2 ± 276.7 (0.569)	3374.3 ± 282.6 (<0.001*)
Anterior hippocampal volume[a] (mm^3)	1455.5 ± 195.8	1453.1 ± 165.4 (0.943)	1430.8 ± 178.4 (0.529)	1718.5 ± 202.2 (<0.001*)
Posterior hippocampal volume[a] (mm^3)	1435.6 ± 162.5	1350.7 ± 161.9 (0.006*)	1426.4 ± 137.9 (0.768)	1655.9 ± 152.6 (<0.001*)
Anterior to posterior hippocampal volume ratio	1.021 ± 0.142	1.086 ± 0.144 (0.016*)	1.006 ± 0.113 (0.578)	1.044 ± 0.134 (0.327)
ERC cortical thickness[b] (mm)	1.967 ± 0.219[c]	1.944 ± 0.143[d] (0.539)	1.922 ± 0.191[e] (0.304)	2.053 ± 0.142[f] (0.018*)
BA35 cortical thickness[b] (mm)	2.189 ± 0.212[c]	2.160 ± 0.197[d] (0.452)	2.174 ± 0.228[e] (0.758)	2.315 ± 0.153[f] (0.001*)
BA36 cortical thickness[b] (mm)	2.351 ± 0.198[c]	2.309 ± 0.199[d] (0.265)	2.326 ± 0.259[e] (0.605)	2.371 ± 0.219[f] (0.592)
PHC cortical thickness[b] (mm)	2.078 ± 0.150[c]	2.088 ± 0.138[d] (0.731)	2.086 ± 0.145[e] (0.812)	2.129 ± 0.129[f] (0.030*)
Log WMH[a]	1.52 ± 1.13	1.51 ± 1.11 [g] (0.935)	0.84 ± 1.07 [h] (0.004*)	1.07 ± 1.09[i] (0.017*)

Data presented as mean ± standard deviation (p-value) and compared to mismatch MCI group with Independent Sample T-Tests. a. adjusted for age and intracranial volume. b. adjusted for age. c. n = 43. d. n = 81. e. n = 46. f. n = 160. g. n = 82. h. n = 44. i. n = 140. T-tau, total tau; p-tau, phosphorylated tau; Aß42, ß-amyloid 1–42; ERC, entorhinal cortex; BA35, Brodmann area 35; BA36, Brodmann area 36; PHC, parahippocampal cortex; mismatch MCI, A + T-(N +) MCI; prodromal AD, A + T+ (N +) MCI; neurodegeneration-only MCI, A-T-(N +) MCI; A- CN, Amyloid-negative cognitively normal controls. *p < 0.05.

longitudinal volume change in the anterior hippocampus, posterior hippocampus, ERC, BA35, BA36, and PHC. The models incorporate baseline age, baseline volume, group, time, and time*group interaction as fixed effects. Time*group interaction terms differed significantly ($p < 0.001$) for all regions, indicating different atrophy rates amongst the four groups. Supplemental Table 3 contains the time*group interaction estimates, standard errors, and p-values for mixed effects models with the same parameters comparing mismatch MCI to each of the other groups individually. These comparisons showed that the prodromal AD group had higher atrophy rates than mismatch MCI in all included regions ($p < 0.005$), while neurodegeneration-only MCI and A- CN had slower rates of atrophy than mismatch MCI in all included regions ($p < 0.05$) except BA36, where atrophy rates were comparable. There were no significant differences between mismatch MCI and the other groups in longitudinal volume change rates for WMHs. Supplemental Table 4 displays the number of participants in each group who underwent MRI at baseline and at each follow-up time point and who met inclusion criteria for the longitudinal imaging analysis.

3.3.3. Longitudinal CSF biomarkers

To determine the stability of the T- status of the mismatch MCI and neurodegeneration-only MCI groups, we examined CSF p-tau at 24 and 48 months from baseline. Mismatch MCI and neurodegeneration-only MCI had similarly low rates of becoming T+ at 24 months (mismatch MCI: 2/20; neurodegeneration-only MCI: 4/20; $p = 0.661$) and 48 months (mismatch MCI: 0/9; neurodegeneration-only MCI: 2/12; $p = 0.486$).

3.3.4. Amyloid and tau PET scans

Tau burden over time was further assessed using publicly available processed tau PET data with flortaucipir from ADNI (see Table 4). Due to the later incorporation of tau PET in the ADNI protocol these scans were acquired a number of years after the baseline of the present study (~5 years). Mean SUVR values in Braak I/II, III/IV and V/VI were examined. Note that, based on prior work, an SUVR cut-off of 1.26 in the Braak III/IV region has been used to define tau positivity (Harrison et al., 2020), and an SUVR cut-off of 1.11 in a composite amyloid region has been used to define amyloid positivity (Schreiber et al., 2015). The mean SUVR in Braak III/IV for mismatch MCI was below this cutoff (1.18 ± 0.21) for T+ despite the tau PET scan occurring approximately five years after the initial T- designation, based on CSF p-tau. Further, this was significantly lower than the prodromal AD group (1.57 ± 0.52, $p = 0.013$), but did not differ from the neurodegeneration-only MCI or preclinical AD group. As an alternative means to quantify amyloid burden, we also examined amyloid PET SUVRs in a composite region. These scans were obtained at the baseline of this study with florbetapir PET. While still above the typical cutoff for being "amyloid positive" (i.e. 1.11) the mean SUVR of the mismatch group (1.21 ± 0.18) was significant lower than the prodromal AD group (1.45 ± 0.18, $p < 0.001$) despite no difference in CSF Aß42 at baseline. The amyloid PET composite SUVR did not differ significantly between the mismatch MCI and preclinical AD groups.

4. Discussion

In this study, we utilized the NIA-AA A/T/(N) research framework (Jack et al., 2018) to compare mismatch MCI [A+T-(N+) MCI] to prodromal AD [A+T+(N+) MCI] on cross-sectional and longitudinal cognition and imaging characteristics with the expectation that mismatch MCI would be less "AD-like" and demonstrate features suggestive of non-AD pathology. This hypothesis was motivated by the notion that neurodegeneration and cognitive decline are driven by tau-based neurofibrillary tangle pathology on the AD continuum. As such, individuals with evidence of neurodegeneration and cognitive impairment in the absence of tau are likely to have a non-AD process effecting these changes, regardless of the presence of β-amyloid. Thus, we also compared mismatch MCI to neurodegeneration-only MCI [A-T-(N+) MCI], which is also thought to result from non-AD pathology.

Compared to prodromal AD, the mismatch MCI group did, indeed, display characteristics that differed from a canonical "AD-like" cognitive profile. In particular, the mismatch group displayed less episodic memory impairment, as measured by verbal recall, but performed similarly on executive function, as measured by the Trail Making Test. Differences in the pattern of cognitive impairment between the mismatch and prodromal AD groups argue against the notion that the mismatch MCI group is simply earlier in the disease process than prodromal AD. Nonetheless, overall cognitive performance of the mismatch group was generally intermediate between prodromal AD and the neurodegeneration-only group. If the assumption is that the cognitive symptoms of the mismatch and neurodegeneration-only groups are primarily driven by non-AD pathology, it is unclear why mismatch MCI was more impaired at baseline. While the β-amyloid in mismatch MCI is thought to be in a preclinical stage (given normal CSF p-tau), its presence may have some bearing on the relative likelihood or distributions of other non-AD pathologies, such as amyloid angiopathy and alpha-synuclein (Swirski et al., 2014; Charidimou et al., 2018; Bassil et al., 2020). Additionally, the neurodegeneration-only group may be relatively enriched in individuals without neurodegenerative pathology, as some individuals with the A-T-(N+) biomarker status may have physiologically small hippocampi and sufficiently impaired cognitive test performance to qualify for an MCI diagnosis in ADNI without actually having a progressive syndrome.

The longitudinal cognitive data provided a clearer contrast between mismatch MCI and prodromal AD. Across all four cognitive measures, the prodromal AD group displayed greater rates of decline compared to

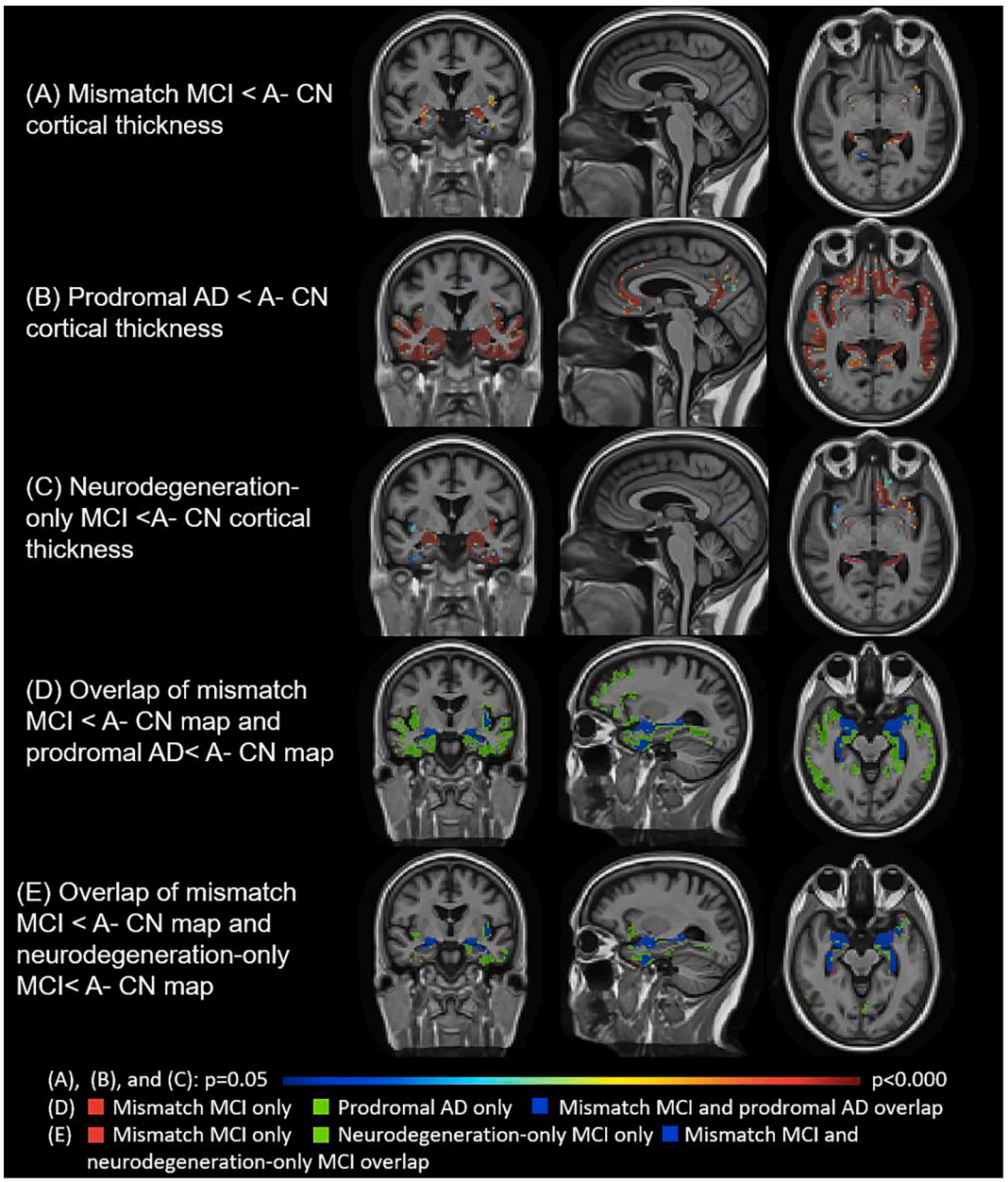

Fig. 1. Cortical regions with significantly reduced cortical thickness in three MCI groups compared to A- CN at baseline ($p < 0.05$, FWE-corrected), and overlap maps. (A), (B), (C): Shaded regions represent areas, based on familywise-error-corrected p-values, with age, sex, and education as covariates, where (A) mismatch MCI, (B) prodromal AD, or (C) neurodegeneration-only MCI have lower mean cortical thickness than A- CN when adjusting for age, sex, and education. (D) and (E): Shaded regions represent overlap of cortical thickness maps for (D) mismatch MCI < A- CN and prodromal AD < A- CN and (E) mismatch MCI < A- CN and neurodegeneration-only MCI < A- CN ($p < 0.05$). Mismatch MCI, A+T-(N+) MCI; prodromal AD, A+T+(N+) MCI; neurodegeneration-only MCI, A-T-(N+) MCI; A-CN, amyloid-negative cognitively normal controls.

mismatch MCI. The trajectory of the mismatch group was essentially the same as the neurodegeneration-only group, with minimal change over the four-year period. Thus, regarding the rate of decline in longitudinal cognition, the mismatch group appears to be more similar to the neurodegeneration-only group than the prodromal AD group.

The neuroimaging data also provides insight into potential differences between the groups. While the MCI groups displayed similar degrees of reduced hippocampal volume, the patterns of atrophy along the long axis of the hippocampus differed. The three groups had highly similar anterior hippocampal volumes, but the prodromal AD group had significantly greater posterior hippocampal atrophy compared to mismatch MCI which, in turn, did not differ from neurodegeneration-only MCI. We also found that the anterior-to-posterior-hippocampal-volume ratio was lower in the two T- groups than the prodromal AD group. This finding, while post-hoc, is intriguing, as one potential source of non-AD hippocampal atrophy is TDP-43, or LATE (Nelson et al., 2019). Prior work has suggested that a distinction between the pattern of tau-based neurofibrillary tangle pathology and TDP-43 is that the former has a more uniform atrophy pattern along the long axis of the hippocampus, if not a greater predilection for the posterior hippocampus, while TDP-43 pathology has been associated with relatively greater involvement of the anterior hippocampus (Lladó et al., 2018; de Flores et al., 2020). Disproportionate anterior hippocampal involvement, relative to the posterior hippocampus, in the T- groups supports the notion that some proportion of the mismatch and neurodegeneration-only groups may have TDP-43 pathology.

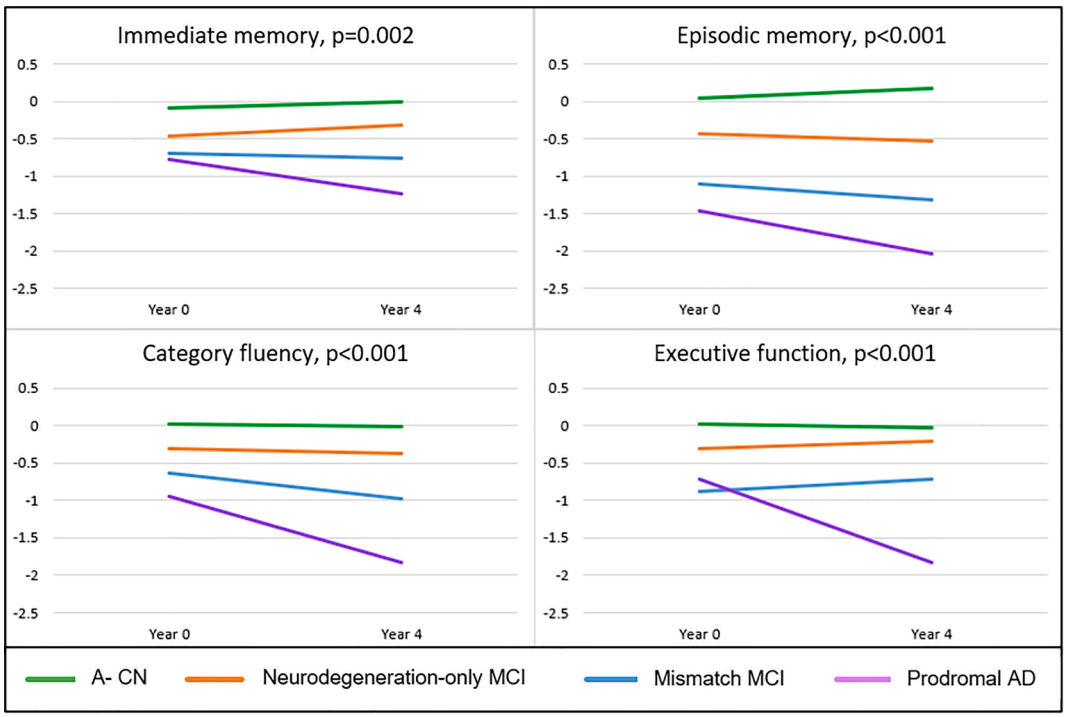

Fig. 2. Mixed effects models of longitudinal cognition Z-scores for up to four years of follow-up. Unadjusted baseline and longitudinal Z-scores, referenced to 161 A- CN baseline scores, were analyzed with mixed effects models, incorporating baseline age, sex, education, baseline test performance, baseline group assignment, time, and time*group interaction as fixed effects, for each included cognitive domain for each participant's cognitive testing. Sex was not significant and was not incorporated into the figures. P-values are for the time*group interaction term for models incorporating all four participant groups simultaneously. Immediate memory, episodic memory, category fluency, and executive function were determined using RAVLT trial 1, RAVLT 5-minute delayed recall, the animal naming test, and negative natural log of Trails B minus Trails A, respectively. A- CN, amyloid-negative cognitively normal; neurodegeneration-only MCI, A-T-(N+) MCI; mismatch MCI, A+T-(N+) MCI; prodromal AD, A+T+(N+) MCI.

The mismatch group also displayed elevated WMH burden relative to A- CN at baseline but did not differ from the prodromal AD group. Cerebrovascular disease may be associated with hippocampal atrophy and is another important driver of age-related cognitive decline, particularly in the domain of executive function (Fiford et al., 2017; Wolk et al., 2018; Caillaud et al., 2020; Puzo et al., 2019). The finding that mismatch MCI had a burden of WMHs that was similar to prodromal AD, but significantly greater than that of the neurodegeneration-only MCI group, also may suggest the possibility that some degree of WMH burden in both groups was driven by amyloid angiopathy, a frequent co-occurrence with cerebral amyloid and similar driver of cognitive decline (Greenberg et al., 2020). The presence of β-amyloid may have driven cognitive decline in some portion of the mismatch group, via the mechanism of cerebral amyloid angiopathy or other β-amyloid-related mechanism, particularly in light of the mismatch group's somewhat disproportionate executive dysfunction relative to episodic memory impairment compared to prodromal AD (Case et al., 2016).

Longitudinal analysis of MTL structures also revealed differences between the MCI groups, such that the mismatch MCI group had slower rates of atrophy than prodromal AD in all selected regions. Conversely, mismatch MCI had faster rates of atrophy than neurodegeneration-only MCI in most selected MTL regions. While it is not clear why the mismatch group would have greater atrophy rates in the absence of tau pathology if neurodegeneration is driven by non-AD pathology in both groups, this finding may suggest that concomitant AD pathophysiology has synergistic effects in the mismatch group or that some portion of the neurodegeneration-only MCI group lacks a neurodegenerative process. Finally, the finding that mismatch MCI had faster atrophy rates compared to controls suggests that the mismatch group had neurodegeneration beyond age-related change.

The whole-brain analyses demonstrated marked differences between the baseline atrophy patterns of mismatch MCI and prodromal AD, compared to A- CN – specifically that cortical thinning in mismatch MCI was relatively restricted to the MTL while prodromal AD had widespread cortical thinning affecting the temporal, frontal, and parietal lobes, consistent with typical AD signature regions (Dickerson et al., 2009). While these differences could reflect the mismatch MCI group simply being at an earlier phase of the same disease process as prodromal AD, the finding that MTL atrophy rates were slower in the former despite "starting" at the same place in the baseline analysis argues otherwise. The finding that the mismatch MCI map overlaps much more so with neurodegeneration-only MCI map than the prodromal AD map further supports the concept that both the mismatch and neurodegeneration-only groups reflect a non-AD pathologic process.

The finding that, in some cases, the mismatch group was intermediate between the prodromal AD and neurodegeneration-only groups does raise the possibility that mismatch MCI is simply prodromal AD at an earlier stage, perhaps sampled just before "converting" to tau positivity or reflecting lower levels of tau just below the threshold of our CSF measure. While possible, several factors make this explanation less likely, at least for a significant proportion of the mismatch group.

First, of the limited number of the mismatch MCI group who underwent repeat LP, only 2/20 at two years and 0/9 at four years converted to tau-positivity (based on CSF p-tau). While most members of the mismatch MCI group would be expected to become tau-positive eventually, this transition is expected to occur many years after initially becoming β-amyloid-positive and would not explain the cognitive or neurodegeneration status of individuals in the mismatch MCI group during the study period unless the transition to tau-positivity occurred early on. While firm conclusions cannot be drawn based on this limited subset of participants who underwent repeat LP, particularly at 48 months, one would expect that if this group reflected subthreshold tau, a greater percentage would have passed this threshold over this timeframe. Similarly, the tau PET data demonstrates that the mean SUVR in

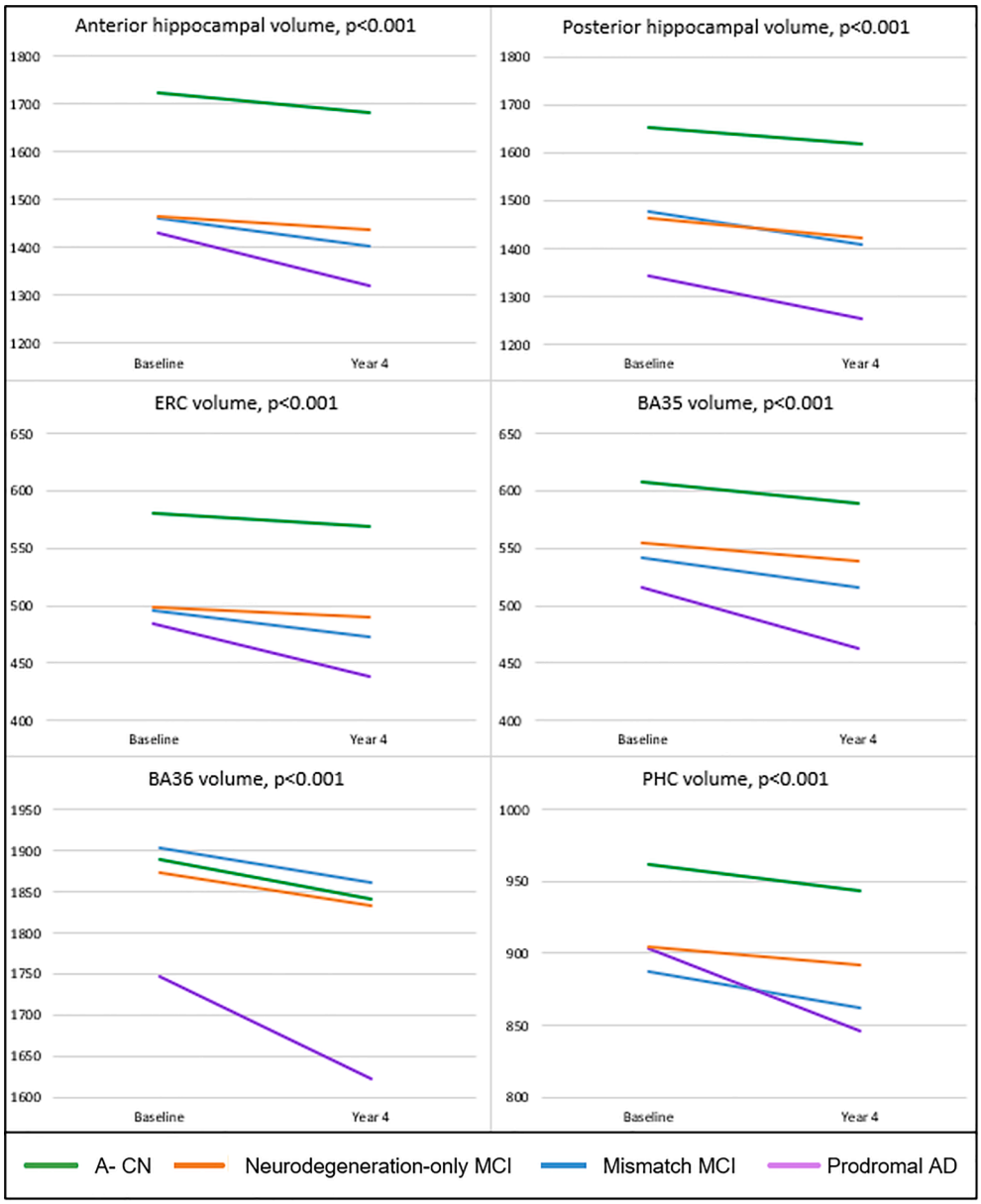

Fig. 3. Mixed effects models of baseline and longitudinal hippocampal and extra-hippocampal MTL structure volumes for up to four years of follow-up. Mixed effects models incorporating baseline age, baseline volume, group, time, and time*group interaction were run to compare each group's baseline and longitudinal volumes over time for anterior hippocampus, posterior hippocampus, ERC, BA35, BA36, and PHC. P-values are for the time*group interaction term for each model in which all four participant groups were included simultaneously. Volumes (y-axis) are in cubic millimeters. ERC, entorhinal cortex; BA35, Brodmann Area 35; BA36, Brodmann Area 36; PHC, parahippocampal cortex; A- CN, amyloid-negative controls; neurodegeneration-only MCI, A-T-(N+) MCI; mismatch MCI, A+T-(N+) MCI; prodromal AD, A+T+(N+) MCI.

Table 4
Mean amyloid PET composite SUVR and Tau PET SUVR in Braak regions.

	Mismatch MCI (n = 44, 16)	Prodromal AD (n = 84, 16)	Neuro-degeneration-only MCI (n = 46, 18)	A- CN (n = 161, 81)	Preclinical AD (n = 88, 42)
Amyloid PET composite SUVR	1.21 ± 0.18	1.45 ± 0.18 (<0.001*)	1.02 ± 0.07 (<0.001*)	1.05 ± 0.12 (<0.001*)	1.26 ± 0.21 (0.136)
Time between baseline and Tau PET (years)	5.3 ± 1.1	5.4 ± 1.1 (0.795)	6.1 ± 1.1 (0.054)	5.0 ± 1.3 (0.336)	4.9 ± 1.3 (0.271)
Braak I/II SUVR	1.20 ± 0.32	1.68 ± 0.48 (0.002*)	1.14 ± 0.26 (0.604)	1.09 ± 0.10 (0.209)	1.20 ± 0.20 (0.898)
Braak III/IV SUVR	1.18 ± 0.21	1.57 ± 0.52 (0.013*)	1.10 ± 0.11 (0187)	1.11 ± 0.09 (0.200)	1.17 ± 0.15 (0.880)
Braak V/VI SUVR	1.08 ± 0.16	1.31 ± 0.35 (0.028*)	1.01 ± 0.09 (0.146)	1.03 ± 0.08 (0.243)	1.07 ± 0.12 (0.774)

Data presented as mean ± standard deviation (p-value) and compared to mismatch MCI group with Independent Sample T-Tests. First *n* value listed is the number of participants with amyloid PET scans; second *n* value is the number of participants with tau PET scans. Mismatch MCI, A+T-(N+) MCI; prodromal AD, A+T+(N+) MCI; neurodegeneration-only MCI, A-T-(N+); A- CN, amyloid-negative cognitively normal; preclinical AD, amyloid-positive cognitively normal. *p < 0.05.

the Braak III/IV region for the mismatch MCI group was below the previously proposed SUVR cut-off for tau positivity an average of five years from baseline. This, too, suggests that most members of the mismatch MCI group at baseline were not on the cusp of becoming tau-positive. Instead, as expected, the mismatch MCI group very closely resembles the preclinical AD group regarding PET-based biomarkers for AD. Interestingly, despite CSF Aß42 levels being essentially the same for the mismatch and prodromal group, amyloid PET at baseline was significantly lower although still in the "positive" range and highly similar to the preclinical AD group. Thus, this group also likely reflects

an earlier stage of amyloid deposition than the prodromal group. While sample sizes for both the tau PET data and longitudinal CSF data are limited, these post-hoc analyses are consistent with the mismatch group containing individuals whose AD pathology is on par with a typical preclinical AD stage and thus whose impaired cognition and neurodegeneration are likely due to alternative causes.

Second, if the cognitive and neurodegenerative status of the mismatch MCI group just reflected "earlier" prodromal AD rather than changes attributable to non-AD pathology, then the mismatch MCI group would be one that lacks resilience, compared to prodromal AD, given symptoms at an earlier pathologic stage of disease. Were this the case, then mismatch MCI would be expected to have faster cognitive decline over time rather than being largely stable. Thus, the presence of alternative non-AD pathology in mismatch MCI remains the best explanation for this group's characteristics.

The findings that the mismatch MCI group had a higher percentage of males and a lower rate of ApoE4 carriership compared to prodromal AD are of uncertain significance but do support the notion that there are biological differences between the groups and argue against the idea that mismatch MCI is merely prodromal AD at an earlier stage.

This study had several limitations. While the overall size of the MCI cohort was reasonably large, the different groups were still modest in size. Additionally, the use of a single neuropsychological test to evaluate each included cognitive domain, a strategy employed to simplify and streamline the analysis, may not fully quantify the true degree of impairment in each domain for each participant. Further, while at a group level the findings have implications for the underlying etiology of cognitive impairment and prognosis, conclusions at a single subject level are difficult to draw. It is certainly possible that some proportion of the mismatch group had early tau pathology below threshold detection that was an important driver of symptoms and progression. That said, the presence of cerebral β-amyloid, even in the presence of neurodegeneration, without evidence of tau pathology is likely to be associated with a more indolent course.

The lack of pathologic validation with autopsy data limits our ability to draw definitive conclusions regarding the pathologic underpinnings of the biomarker-defined MCI groups. The ADNI MCI cohort, which is restricted to amnestic-predominant cases with low Modified Hachinski Ischemic scores and has limited racial, socioeconomic, and educational diversity, does not represent the full breadth of MCI.

The A/T/(N) model allows researchers to select from several different methods for defining each of the three binary biomarkers, and, therefore, our choices regarding biomarker selection and cut-offs influenced the composition of the groups and the results. It is possible that selection of a neurodegeneration biomarker that was less specific for AD pathology than hippocampal volume might have led to a more inclusive and larger mismatch MCI group with stronger indicators of non-AD pathologies. Similarly, the exclusion of MCI cases that were non-amnestic or that had elevated Hachinski scores (indicating higher likelihood of a vascular etiology for cognitive symptoms) may also have blunted the strength of the conclusions, as one would expect the excluded MCI cases to fall disproportionately into the mismatch MCI and neurodegeneration-only MCI groups, rather than the prodromal AD group, and potentially contribute to making these T- MCI groups differ more markedly from the prodromal AD group in ways that might have been more strongly suggestive of non-AD pathologies. Further, the exclusion of participants who were likely to have significant cerebrovascular disease restricts the sample and compromises our ability to draw conclusions about the role of cerebrovascular disease as a non-AD pathologic driver in some cases of MCI. These points and the lack of diversity in the ADNI cohort limit the generalizability of the findings.

5. Conclusions

The current work is largely consistent with several recent studies that have demonstrated generally poorer prognoses in groups with positive A, T, and N biomarkers relative to other groups (Burnham et al., 2019; Jack et al., 2019; Yu et al., 2019). We extend these prior findings by providing support for the notion that the relative presence or absence of A/T/(N) biomarkers may provide insights into underlying drivers of cognitive impairment in MCI. In particular, we focused on mismatch MCI, an A+ group defined by neurodegeneration in the absence of tau pathology and found that this group differed from prodromal AD on cross-sectional and longitudinal cognitive and imaging measures. Indeed, the mismatch group overlapped to a greater extent with the neurodegeneration-only MCI group. These findings suggest that among β-amyloid-positive neurodegeneration-positive MCI, tau status is an important biomarker that can parse out two groups: one that can be expected to have a consistent "AD-like" decline in cognition, with correspondingly faster brain atrophy rates, and one that can be expected to decline slowly, both with regard to cognitive change and brain atrophy. The differences in cognition and imaging characteristics between mismatch MCI and prodromal AD are best explained by differences in underlying disease processes, with prodromal AD proceeding through the classical stages (Shaw) of AD, and mismatch MCI being a group that may be heterogenous with regard to various non-AD pathologies with concomitant preclinical AD, but overall represents a more indolent category of MCI. Given the critical role of tau pathology in the cognitive and neurodegenerative phenotype of AD, we propose that this mismatch group reflects individuals with non-AD causes of their MCI status. The current findings have relevance for enrollment in clinical trials of such "mismatch" patients in light of the potential differences in underlying pathologies and prognosis from prodromal AD. These results also have relevance for clinical care in light of the prognostic implications. Future directions for this research include the use of amyloid and tau PET scans, rather than CSF Aß42 and p-tau, to define amyloid and tau status. This less-invasive approach provides information about the anatomic distribution of amyloid and tau accumulation and is now feasible using ADNI data as an ever-growing number of participants have undergone these scans.

6. Data availability

ADNI data is publicly available and can be accessed for download by visiting the ADNI website (http://adni.loni.usc.edu/). Processed ADNI data will be provided upon request by the corresponding author.

Funding

This work was supported by a grant from the Alzheimer's Association [grant number 2019-AACSF-642998]. Additional funding sources include ADRC AG010124, R01 AG056014, and R01 AG055005.

CRediT authorship contribution statement

Lauren E. McCollum: Conceptualization, Formal analysis, Writing - original draft, Visualization, Funding acquisition. **Sandhitsu R. Das:** Software, Validation, Formal analysis, Data curation, Writing - review & editing. **Long Xie:** Methodology, Software, Data curation, Writing - review & editing. **Robin Flores:** Methodology, Software, Data curation, Writing - review & editing. **Jieqiong Wang:** Software, Writing - review & editing. **Sharon X. Xie:** Supervision, Writing - review & editing. **Laura E.M. Wisse:** Methodology, Writing - review & editing. **Paul A. Yushkevich:** Methodology, Software, Writing - review & editing, Supervision, Funding acquisition. **David A. Wolk:** Conceptualization, Methodology, Writing - review & editing, Supervision, Funding acquisition.

Acknowledgements

Data collection and sharing for this project was funded by ADNI (National Institutes of Health Grant U01 AG024904) and DOD ADNI

(Department of Defense award number W81XWH-12-2-0012). ADNI is funded by the National Institute on Aging, the National Institute of Biomedical Imaging and Bioengineering, and through generous contributions from the following: AbbVie, Alzheimer's Association; Alzheimer's Drug Discovery Foundation; Araclon Biotech; BioClinica, Inc.; Biogen; Bristol-Myers Squibb Company; CereSpir, Inc.;Cogstate;Eisai Inc.; Elan Pharmaceuticals, Inc.; Eli Lilly and Company; EuroImmun; F. Hoffmann-La Roche Ltd and its affiliated company Genentech, Inc.; Fujirebio; GE Healthcare; IXICO Ltd.; Janssen Alzheimer Immunotherapy Research & Development, LLC.; Johnson & Johnson Pharmaceutical Research & Development LLC.; Lumosity; Lundbeck; Merck & Co., Inc.; Meso Scale Diagnostics, LLC.;NeuroRx Research; Neurotrack Technologies;Novartis Pharmaceuticals Corporation; Pfizer Inc.; Piramal Imaging; Servier; Takeda Pharmaceutical Company; and Transition Therapeutics. The Canadian Institutes of Health Research is providing funds to support ADNI clinical sites in Canada. Private sector contributions are facilitated by the Foundation for the National Institutes of Health (www.fnih.org). The grantee organization is the Northern California Institute for Research and Education, and the study is coordinated by the Alzheimer's Therapeutic Research Institute at the University of Southern California. ADNI data are disseminated by the Laboratory for Neuro Imaging at the University of Southern California.

Appendix A. Supplementary data

Supplementary data to this article can be found online at https://doi.org/10.1016/j.nicl.2021.102717.

References

Abner, E.L., Kryscio, R.J., Schmitt, F.A., Fardo, D.W., Moga, D.C., Ighodaro, E.T., Jicha, G.A., Yu, L., Dodge, H.H., Xiong, C., Woltjer, R.L., Schneider, J.A., Cairns, N. J., Bennett, D.A., Nelson, P.T., 2017. Outcomes after diagnosis of mild cognitive impairment in a large autopsy series. Ann. Neurol. 81 (4), 549–559.

Bassil, F., Brown, H.J., Pattabhiraman, S., Iwasyk, J.E., Maghames, C.M., Meymand, E.S., et al., 2020. Amyloid-Beta (Abeta) plaques promote seeding and spreading of alpha-synuclein and tau in a mouse model of lewy body disorders with abeta pathology. Neuron 105 (2), 260–75 e6.

Binetti, G., Magni, E., Cappa, S.F., Padovani, A., Bianchetti, A., Trabucchi, M., 1995. Semantic memory in Alzheimer's disease: An analysis of category fluency. J. Clin. Exp. Neuropsychol. 17 (1), 82–89.

Bittner, T., Zetterberg, H., Teunissen, C.E., Ostlund Jr., R.E., Militello, M., Andreasson, U., et al., 2016. Technical performance of a novel, fully automated electrochemiluminescence immunoassay for the quantitation of beta-amyloid (1–42) in human cerebrospinal fluid. Alzheimers Dement 12 (5), 517–526.

Blennow, K., Shaw, L.M., Stomrud, E., Mattsson, N., Toledo, J.B., Buck, K., et al., 2019. Predicting clinical decline and conversion to Alzheimer's disease or dementia using novel Elecsys Abeta(1–42), pTau and tTau CSF immunoassays. Sci. Rep. 9 (1), 19024.

Boyle, P.A., Yang, J., Yu, L., Leurgans, S.E., Capuano, A.W., Schneider, J.A., et al., 2017. Varied effects of age-related neuropathologies on the trajectory of late life cognitive decline. Brain 140 (3), 804–812.

Braak, H., Braak, E., 1991. Neuropathological stageing of Alzheimer-related changes. Acta Neuropathol. 82 (4), 239–259.

Burnham, S.C., Coloma, P.M., Li, Q.X., Collins, S., Savage, G., Laws, S., et al., 2019. Application of the NIA-AA Research Framework: Towards a biological definition of Alzheimer's disease using cerebrospinal fluid biomarkers in the AIBL Study. J. Prev. Alzheimers Dis. 6 (4), 248–255.

Caillaud M, Hudon C, Boller B, Brambati S, Duchesne S, Lorrain D, et al. Evidence of a Relation Between Hippocampal Volume, White Matter Hyperintensities, and Cognition in Subjective Cognitive Decline and Mild Cognitive Impairment. J Gerontol B Psychol Sci Soc Sci 2019.

Carriere I, Fourrier-Reglat A, Dartigues JF, Rouaud O, Pasquier F, Ritchie K, et al. Drugs with anticholinergic properties, cognitive decline, and dementia in an elderly general population: the 3-city study. Arch Intern Med 2009; 169(14): 1317-24.

Case, N.F., Charlton, A., Zwiers, A., Batool, S., McCreary, C.R., Hogan, D.B., Ismail, Z., Zerna, C., Coutts, S.B., Frayne, R., Goodyear, B., Haffenden, A., Smith, E.E., 2016. Cerebral amyloid angiopathy is associated with executive dysfunction and mild cognitive impairment. Stroke 47 (8), 2010–2016.

Charidimou, A., Friedrich, J.O., Greenberg, S.M., Viswanathan, A., 2018. Core cerebrospinal fluid biomarker profile in cerebral amyloid angiopathy: A meta-analysis. Neurology 90 (9), e754–e762.

Corrigan, J.D., Hinkeldey, N.S., 1987. Relationships between parts A and B of the Trail Making Test. J. Clin. Psychol. 43 (4), 402–409.

Cousins, K.A.Q., Phillips, J.S., Irwin, D.J., Lee, E.B., Wolk, D.A., Shaw, L.M., Zetterberg, H., Blennow, K., Burke, S.E., Kinney, N.G., Gibbons, G.S., McMillan, C.T., Trojanowski, J.Q., Grossman, M., 2021. ATN incorporating cerebrospinal fluid neurofilament light chain detects frontotemporal lobar degeneration. Alzheimers Dement 17 (5), 822–830.

Dadar, M., Maranzano, J., Misquitta, K., Anor, C.J., Fonov, V.S., Tartaglia, M.C., Carmichael, O.T., Decarli, C., Collins, D.L., 2017. Performance comparison of 10 different classification techniques in segmenting white matter hyperintensities in aging. Neuroimage 157, 233–249.

Das, S.R., Avants, B.B., Grossman, M., Gee, J.C., 2009. Registration based cortical thickness measurement. Neuroimage 45 (3), 867–879.

Das, S.R., Avants, B.B., Pluta, J., Wang, H., Suh, J.W., Weiner, M.W., Mueller, S.G., Yushkevich, P.A., 2012. Measuring longitudinal change in the hippocampal formation from in vivo high-resolution T2-weighted MRI. Neuroimage 60 (2), 1266–1279.

Flores, R., Wisse, L.E.M., Das, S.R., Xie, L., McMillan, C.T., Trojanowski, J.Q., Robinson, J.L., Grossman, M., Lee, E., Irwin, D.J., Yushkevich, P.A., Wolk, D.A., 2020. Contribution of mixed pathology to medial temporal lobe atrophy in Alzheimer's disease. Alzheimers Dement 16 (6), 843–852.

Dickerson BC, Bakkour A, Salat DH, Feczko E, Pacheco J, Greve DN, et al. The cortical signature of Alzheimer's disease: regionally specific cortical thinning relates to symptom severity in very mild to mild AD dementia and is detectable in asymptomatic amyloid-positive individuals. Cereb Cortex 2009; 19(3): 497-510.

Fiford, C.M., Manning, E.N., Bartlett, J.W., Cash, D.M., Malone, I.B., Ridgway, G.R., Lehmann, M., Leung, K.K., Sudre, C.H., Ourselin, S., Biessels, G.J., Carmichael, O.T., Fox, N.C., Cardoso, M.J., Barnes, J., 2017. White matter hyperintensities are associated with disproportionate progressive hippocampal atrophy. Hippocampus 27 (3), 249–262.

Gordon, B.A., Blazey, T., Su, Y., Fagan, A.M., Holtzman, D.M., Morris, J.C., et al., 2016. Longitudinal beta-Amyloid deposition and hippocampal volume in preclinical alzheimer disease and suspected non-alzheimer disease pathophysiology. JAMA Neurol. 73 (10), 1192–1200.

Greenberg, S.M., Bacskai, B.J., Hernandez-Guillamon, M., Pruzin, J., Sperling, R., van Veluw, S.J., 2020. Cerebral amyloid angiopathy and Alzheimer disease - one peptide, two pathways. Nat. Rev. Neurol. 16 (1), 30–42.

Harrison, T.M., Du, R., Klencklen, G., Baker, S.L., Jagust, W.J., 2020. Distinct effects of beta-amyloid and tau on cortical thickness in cognitively healthy older adults. Alzheimers Dement.

Jack, C.R., Bennett, D.A., Blennow, K., Carrillo, M.C., Dunn, B., Haeberlein, S.B., Holtzman, D.M., Jagust, W., Jessen, F., Karlawish, J., Liu, E., Molinuevo, J.L., Montine, T., Phelps, C., Rankin, K.P., Rowe, C.C., Scheltens, P., Siemers, E., Snyder, H.M., Sperling, R., Elliott, C., Masliah, E., Ryan, L., Silverberg, N., 2018. NIA-AA Research Framework: Toward a biological definition of Alzheimer's disease. Alzheimers Dement 14 (4), 535–562.

Jack, C.R., Knopman, D.S., Weigand, S.D., Wiste, H.J., Vemuri, P., Lowe, V., Kantarci, K., Gunter, J.L., Senjem, M.L., Ivnik, R.J., Roberts, R.O., Rocca, W.A., Boeve, B.F., Petersen, R.C., 2012. An operational approach to National Institute on Aging-Alzheimer's Association criteria for preclinical Alzheimer disease. Ann. Neurol. 71 (6), 765–775.

Jack, C.R., Wiste, H.J., Therneau, T.M., Weigand, S.D., Knopman, D.S., Mielke, M.M., Lowe, V.J., Vemuri, P., Machulda, M.M., Schwarz, C.G., Gunter, J.L., Senjem, M.L., Graff-Radford, J., Jones, D.T., Roberts, R.O., Rocca, W.A., Petersen, R.C., 2019. Associations of amyloid, tau, and neurodegeneration biomarker profiles with rates of memory decline among individuals without dementia. JAMA 321 (23), 2316. https://doi.org/10.1001/jama.2019.7437.

Jack Jr., C.R., Wiste, H.J., Weigand, S.D., Therneau, T.M., Knopman, D.S., Lowe, V., et al., 2017. Age-specific and sex-specific prevalence of cerebral beta-amyloidosis, tauopathy, and neurodegeneration in cognitively unimpaired individuals aged 50–95 years: A cross-sectional study. Lancet Neurol. 16 (6), 435–444.

Jicha, G.A., Parisi, J.E., Dickson, D.W., Johnson, K., Cha, R., Ivnik, R.J., Tangalos, E.G., Boeve, B.F., Knopman, D.S., Braak, H., Petersen, R.C., 2006. Neuropathologic outcome of mild cognitive impairment following progression to clinical dementia. Arch. Neurol. 63 (5), 674. https://doi.org/10.1001/archneur.63.5.674.

Landau, S.M., Fero, A., Baker, S.L., Koeppe, R., Mintun, M., Chen, K., et al., 2015. Measurement of longitudinal beta-amyloid change with 18F-florbetapir PET and standardized uptake value ratios. J. Nucl. Med. 56 (4), 567–574.

Lladó, A., Tort-Merino, A., Sánchez-Valle, R., Falgàs, N., Balasa, M., Bosch, B., Castellví, M., Olives, J., Antonell, A., Hornberger, M., 2018. The hippocampal longitudinal axis-relevance for underlying tau and TDP-43 pathology. Neurobiol. Aging 70, 1–9.

Mendez, M.F., Cherrier, M.M., Perryman, K.M., 1997. Differences between Alzheimer's disease and vascular dementia on information processing measures. Brain Cogn. 34 (2), 301–310.

Moradi, E., Hallikainen, I., Hänninen, T., Tohka, J., 2017. Alzheimer's Disease Neuroimaging I. Rey's Auditory Verbal Learning Test scores can be predicted from whole brain MRI in Alzheimer's disease. Neuroimage Clin. 13, 415–427.

Nelson PT, Dickson DW, Trojanowski JQ, Jack CR, Boyle PA, Arfanakis K, et al. Limbic-predominant age-related TDP-43 encephalopathy (LATE): consensus working group report. Brain 2019; 142(6): 1503-27.

Petersen, R.C., 2004. Mild cognitive impairment as a diagnostic entity. J. Intern. Med. 256 (3), 183–194.

Petersen, R.C., 2016. Mild Cognitive Impairment. Continuum (Minneap Minn) 22 (2, Dementia), 404–418.

Pillai, J.A., Butler, R.S., Bonner-Jackson, A., Leverenz, J.B., 2016. Impact of Alzheimer's Disease, lewy body and vascular co-pathologies on clinical transition to dementia in a national autopsy cohort. Dement. Geriatr. Cogn. Disord. 42 (1–2), 106–116.

Prins, N.D., Scheltens, P., 2015. White matter hyperintensities, cognitive impairment and dementia: An update. Nat. Rev. Neurol. 11 (3), 157–165.

Puzo, C., Labriola, C., Sugarman, M.A., Tripodis, Y., Martin, B., Palmisano, J.N., Steinberg, E.G., Stein, T.D., Kowall, N.W., McKee, A.C., Mez, J., Killiany, R.J., Stern, R.A., Alosco, M.L., 2019. Independent effects of white matter hyperintensities on cognitive, neuropsychiatric, and functional decline: A longitudinal investigation using the National Alzheimer's Coordinating Center Uniform Data Set. Alzheimers Res. Ther. 11 (1) https://doi.org/10.1186/s13195-019-0521-0.

Schöll, M., Lockhart, S., Schonhaut, D., O'Neil, J., Janabi, M., Ossenkoppele, R., Baker, S., Vogel, J., Faria, J., Schwimmer, H., Rabinovici, G., Jagust, W., 2016. PET imaging of tau deposition in the aging human brain. Neuron 89 (5), 971–982.

Schreiber, S., Landau, S.M., Fero, A., Schreiber, F., Jagust, W.J., 2015. Alzheimer's Disease Neuroimaging I. Comparison of visual and quantitative florbetapir F 18 Positron emission tomography analysis in predicting mild cognitive impairment outcomes. JAMA Neurol. 72 (10), 1183–1190.

Schwarz, C., Fletcher, E., DeCarli, C., Carmichael, O., 2009. Fully-automated white matter hyperintensity detection with anatomical prior knowledge and without FLAIR. Inf Process Med. Imag. 21, 239–251.

Shaw L. Implementation of fully automated immunoassays for CSF Aβ1-42, t-tau and p-tau181 in the Alzheimer's Disease Neuroimaging Initiative. [cited; Available from: https://www.alz.washington.edu/NONMEMBER/SPR18/BioMarker/SHAW.pdf.

Shaw, L.M., Vanderstichele, H., Knapik-Czajka, M., Clark, C.M., Aisen, P.S., Petersen, R. C., Blennow, K., Soares, H., Simon, A., Lewczuk, P., Dean, R., Siemers, E., Potter, W., Lee, V.-Y., Trojanowski, J.Q., 2009. Cerebrospinal fluid biomarker signature in Alzheimer's disease neuroimaging initiative subjects. Ann. Neurol. 65 (4), 403–413.

Shaw, L.M., Vanderstichele, H., Knapik-Czajka, M., Figurski, M., Coart, E., Blennow, K., Soares, H., Simon, A.J., Lewczuk, P., Dean, R.A., Siemers, E., Potter, W., Lee, V.-Y., Trojanowski, J.Q., 2011. Qualification of the analytical and clinical performance of CSF biomarker analyses in ADNI. Acta Neuropathol. 121 (5), 597–609.

Smith, S., Nichols, T., 2009. Threshold-free cluster enhancement: Addressing problems of smoothing, threshold dependence and localisation in cluster inference. Neuroimage 44 (1), 83–98.

Swirski, M., Miners, J.S., de Silva, R., Lashley, T., Ling, H., Holton, J., et al., 2014. Evaluating the relationship between amyloid-beta and alpha-synuclein phosphorylated at Ser129 in dementia with Lewy bodies and Parkinson's disease. Alzheimers Res. Ther. 6 (5–8), 77.

Tombaugh, T., 2004. Trail Making Test A and B: normative data stratified by age and education. Arch. Clin. Neuropsychol. 19 (2), 203–214.

Tustison, N.J., Cook, P.A., Klein, A., Song, G., Das, S.R., Duda, J.T., Kandel, B.M., van Strien, N., Stone, J.R., Gee, J.C., Avants, B.B., 2014. Large-scale evaluation of ANTs and FreeSurfer cortical thickness measurements. Neuroimage 99, 166–179.

Wisse, L.E.M., Butala, N., Das, S.R., Davatzikos, C., Dickerson, B.C., Vaishnavi, S.N., Yushkevich, P.A., Wolk, D.A., 2015. Suspected non-AD pathology in mild cognitive impairment. Neurobiol. Aging 36 (12), 3152–3162.

Wolk, D.A., Das, S.R., Mueller, S.G., Weiner, M.W., Yushkevich, P.A., 2017. Alzheimer's Disease Neuroimaging I. Medial temporal lobe subregional morphometry using high resolution MRI in Alzheimer's disease. Neurobiol. Aging 49, 204–213.

Wolk, D.A., Sadowsky, C., Safirstein, B., Rinne, J.O., Duara, R., Perry, R., Agronin, M., Gamez, J., Shi, J., Ivanoiu, A., Minthon, L., Walker, Z., Hasselbalch, S., Holmes, C., Sabbagh, M., Albert, M., Fleisher, A., Loughlin, P., Triau, E., Frey, K., Høgh, P., Bozoki, A., Bullock, R., Salmon, E., Farrar, G., Buckley, C.J., Zanette, M., Sherwin, P. F., Cherubini, A., Inglis, F., 2018. Use of Flutemetamol F 18-Labeled positron emission tomography and other biomarkers to assess risk of clinical progression in patients with amnestic Mild Cognitive Impairment. JAMA Neurol. 75 (9), 1114. https://doi.org/10.1001/jamaneurol.2018.0894.

Xie, L., Pluta, J.B., Das, S.R., Wisse, L.E.M., Wang, H., Mancuso, L., Kliot, D., Avants, B.B., Ding, S.-L., Manjón, J.V., Wolk, D.A., Yushkevich, P.A., 2017. Multi-template analysis of human perirhinal cortex in brain MRI: Explicitly accounting for anatomical variability. Neuroimage 144, 183–202.

Xie, L., Wisse, L.E.M., Pluta, J., de Flores, R., Piskin, V., Manjón, J.V., Wang, H., Das, S. R., Ding, S.-L., Wolk, D.A., Yushkevich, P.A., 2019. Automated segmentation of medial temporal lobe subregions on in vivo T1-weighted MRI in early stages of Alzheimer's disease. Hum. Brain Mapp. 40 (12), 3431–3451.

Yu, J.-T., Li, J.-Q., Suckling, J., Feng, L., Pan, A.n., Wang, Y.-J., Song, B.o., Zhu, S.-L., Li, D.-H., Wang, H.-F., Tan, C.-C., Dong, Q., Tan, L., Mok, V., Aisen, P.S., Weiner, M. M., 2019. Frequency and longitudinal clinical outcomes of Alzheimer's AT(N) biomarker profiles: A longitudinal study. Alzheimers Dement 15 (9), 1208–1217.

Yushkevich, P.A., Pluta, J.B., Wang, H., Xie, L., Ding, S.-L., Gertje, E.C., Mancuso, L., Kliot, D., Das, S.R., Wolk, D.A., 2015. Automated volumetry and regional thickness analysis of hippocampal subfields and medial temporal cortical structures in mild cognitive impairment. Hum. Brain Mapp. 36 (1), 258–287.